Published in final edited form as:
Ultrasound Med Biol. 2012 February ; 38(2): 175–182. doi:10.1016/j.ultrasmedbio.2011.10.019.

SHEAR WAVE DISPERSION MEASURES LIVER STEATOSIS

Christopher T. Barry[*], **Bradley Mills**[†], **Zaegyoo Hah**[†], **Robert A. Mooney**[*], **Charlotte K. Ryan**[*], **Deborah J. Rubens**[*], and **Kevin J. Parker**[†]

[*]School of Medicine and Dentistry, University of Rochester, Rochester, NY, USA

[†]Department of Electrical and Computer Engineering, University of Rochester, Rochester, NY, USA

Abstract

Crawling waves, which are interfering shear wave patterns, can be generated in liver tissue over a range of frequencies. Some important biomechanical properties of the liver can be determined by imaging the crawling waves using Doppler techniques and analyzing the patterns. We report that the dispersion of shear wave velocity and attenuation, that is, the frequency dependence of these parameters, are strongly correlated with the degree of steatosis in a mouse liver model, *ex vivo*. The results demonstrate the possibility of assessing liver steatosis using noninvasive imaging methods that are compatible with color Doppler scanners and, furthermore, suggest that liver steatosis can be separated from fibrosis by assessing the dispersion or frequency dependence of shear wave propagations.

Keywords

Shear wave; Crawling wave; Steatosis; Elastography; Liver fibrosis; Dispersion; Attenuation; Nonalcoholic fatty liver disease; Nonalcoholic steatohepatitis

INTRODUCTION

There is growing concern about nonalcoholic fatty liver disease (NAFLD), a major cause of chronic liver disease. The most serious manifestation, nonalcoholic steatohepatitis (NASH), is an increasingly common cause of end stage liver disease (Wanless and Lentz 1990; Angulo 2002; Schreuder et al. 2008; Dowman et al. 2010). Although NASH is known to be associated with the metabolic syndrome (obesity, insulin resistance and hypertriglyceridemia [Wanless and Lentz 1990; Marchesini et al. 1999; Charlton 2004; Vuppalanchi and Chalasani 2009]), the natural history of NAFLD progressing to NASH is incompletely understood. Because of the increasing incidence of fatty liver disease and also the important role fat (or "steatosis") plays in the evaluation of liver donors for transplantation (Selzner and Clavien 2001; Minervini et al. 2009), it is critically important to improve our ability to diagnose the entire spectrum of NAFLD and to understand its pathophysiology. One essential and needed advance is the development of an inexpensive and easy-to-use instrument that could be widely available for researchers to assess the degree of steatosis in the liver repeatedly, painlessly and noninvasively.

Address correspondence to: Kevin J. Parker, University of Rochester, Hopeman Building 203, P.O. Box 270126, Rochester, NY 14627-0126, USA. kevin.parker@rochester.edu.

The gold standard for assessing the degree of hepatic steatosis is biopsy (Strassburg and Manns 2006). Although the risk of postprocedure bleeding is low and the risk of mortality is estimated to be between 0.01% and 0.1%, biopsy is not always logistically possible (especially in an organ donation setting) and the small amount of tissue procured during biopsy may not reflect the global degree of fatty infiltration. Furthermore, liver biopsies are disliked by patients and are sometimes misinterpreted due to processing artifacts or pathologist error. Therefore, a reliable noninvasive means of fat determination would be quite beneficial.

Ultrasound B-scan imaging is an inexpensive and readily available screening tool for steatosis (as determined by increased diffuse echogenicity due to parenchymal fat inclusions) but the sensitivity ranges from 60%–94% and specificity of 66%–95% in determining hepatic steatosis (Foster et al. 1980; Debongnie et al. 1981). Transient elastography, a technique that measures the velocity of propagation of shear waves through tissue to determine stiffness, has been shown to correlate with histologic stages of liver fibrosis between 3 and 5 (Castera et al. 2008; Palmeri et al. 2008). Transient elastography can be generated by a handheld mechanical vibration source placed over the liver (Sandrin et al. 2003) or by radiation force excitation of shear waves (Sarvazyan et al. 1998; Wang et al. 2009). The shear wave speed is directly proportional to the elastic modulus, which increases with advanced liver fibrosis (Carstensen et al. 2008). However, these methods cannot measure steatosis when the output is a single “stiffness” estimate. In fact, steatosis confounds shear wave measurements of fibrosis by adding a second variable (Yoneda et al. 2010) and this issue is clinically significant given that NASH patients have varying degrees of these two variables. Magnetic resonance imaging (MRI) techniques show promise for assessment of steatosis (Bydder et al. 2008; Ehman 2009; Salameh et al. 2009) but are in the research stage and would likely be more expensive and time-consuming than ultrasound techniques.

Although other methods exist to estimate steatosis such as proton magnetic resonance spectroscopy (^{1}H MRS)(Longo et al. 1995) and bioimpedence (Hessheimer et al. 2009), the former is logistically cumbersome in a clinical setting and the latter requires probes to be placed into the liver, thereby severely limiting its clinical utility because of safety issues. More recently, Sandrin and collaborators (Sasso et al. 2010) have added a proprietary ultrasonic attenuation measurement at 3.5 Mhz to assess liver steatosis and to separate the effects of fat from fibrosis with two measurements (ultrasonic attenuation plus elastography). We agree that two measurements are required to estimate two independent variables, fat and fibrosis. However, we propose to evaluate the dispersion of shear wave properties to achieve this goal.

Dispersion refers to the frequency dependence of the speed of shear waves and attenuation of shear waves in a lossy medium. Generally, the speed of shear waves and the attenuation of shear waves (and other types of acoustic waves) will increase with frequency and can be modeled by a complex wave number (Oestreicher 1951; Blackstock 2000; Carstensen et al. 2008). Whatever the precise mechanisms of loss are in a given medium, the dispersion of attenuation and speed are linked by Kramers-Kronig relations that are based on causality constraints (O’Donnell et al. 1981; Szabo and Wu 2000). With the development of elastographic imaging approaches over the past two decades (Parker et al. 2011), some techniques have been extended to examine dispersion in tissues and pathologies including breast cancer (Tanter et al. 2008), liver fibrosis (Muller et al. 2009), muscle (Hoyt et al. 2007; Chen et al. 2009), normal mammalian livers (Chen et al. 2009) and gelatins (Orescanin and Insana 2010). We believe ours is the first effort to utilize the dispersion properties of elastography to measure steatosis as distinct from fibrosis.

We hypothesize that increasing amounts of fat in the normal liver will increase the dispersion (that is, the frequency dependence or slope) of the speed and attenuation of shear waves, while slightly reducing the speed of sound. Figure 1 illustrates our hypothesis. This is simply the consequence of adding a viscous (and highly lossy) component to the liver, which otherwise would exhibit a strong elastic component with lower dispersion (Carstensen et al. 2008). Furthermore, as dispersion increases, so will shear wave attenuation. In this study, we employ crawling waves (CrWs), which are an interference pattern of shear waves, in the liver. The CrWs can be imaged by a Doppler ultrasound scanner, with high signal-to-noise over a large region-of-interest (ROI) (Wu et al. 2006; Hoyt et al. 2008). The analysis of the crawling wave pattern results in an estimate of the shear wave velocity. When repeated over multiple frequencies from 80 to 300 Hz (or higher in smaller animal livers), the resulting data provide the dispersion estimates that are correlated to steatosis.

THEORY

Wu et al. introduced the concept of crawling waves into the elastography field in 2004 (Wu et al. 2006). Two shear wave sources are placed on the two opposite sides of a sample, driven by sinusoidal signals with slightly offset frequencies. The shear waves from the two sources interact to create interference patterns, which are visualized by the vibration sonoelastography technique. Estimations of local shear velocity can be made from the shear wave propagation pattern and, thus, the shear modulus.

Several approaches have been proposed to estimate local shear velocity from the crawling wave patterns, including a method based on a local spatial frequency estimator (LFE) (Wu et al. 2006), estimation by moving interference pattern arrival times (McLaughlin et al. 2007; Lin et al. 2010) and the local autocorrelation method for both one-dimensional (1-D) (Hoyt et al. 2006) and two-dimensional (2-D) shear velocity recoveries (Hoyt et al. 2008). A study of the concurrence between the last technique and mechanical measurement validated the imaging modality for quantification of soft tissue properties (Zhang et al. 2007).

The CrW technique has been used to depict the elastic properties of biologic tissues including radio-frequency ablated hepatic lesions *in vitro* (Hoyt et al. 2006), human skeletal muscle *in vitro* (Hoyt et al. 2007) and excised human prostate (Castaneda et al. 2009). In this study, we focus on crawling waves in the liver.

The discrete version of the detected vibration amplitude square $|u|^2$ of the interference of plane shear waves in a homogeneous medium is (Wu et al. 2006; Zhang et al. 2007):

$$|u(m,n,r)|^2 = 2e^{-\alpha D}\left[\cosh(2\alpha n T_n) + \cos\left(2knT_n + \Delta knT_n - \Delta k\frac{D}{2} + \Delta\omega r T_r\right)\right], \quad (1)$$

where

- α is the attenuation coefficient of the shear waves in the medium,
- D is the separation of the two sources,
- ω, the angular frequency measured in radians per second, is 2π times the frequency (in *Hz*),
- k, the wave number and measured in radians per meter, is 2π divided by the wavelength λ (in meters),
- $\Delta\omega$ is the frequency difference, Δk is wave number difference between the two waves,

- m, n and r are the spatial vertical index, the spatial lateral (shear wave propagation direction) index and the time index, respectively, and
- T_n and T_r are the spatial sampling interval along the lateral direction and the temporal sampling interval, respectively.

The analysis can also be extended for unequal strengths of the two opposing shear waves. Using MAT-LAB computational software (The Mathworks, Inc., Natick, MA, USA) the data are fit to determine the unknown k and α. Thus, the shear velocity v_{shear} is calculated based on the relationship:

$$v_{shear}=\frac{\omega}{k}, \quad (2)$$

where k is the wave number with the unit of m^{-1}. In nearly incompressible soft tissues the relationship between shear wave velocity and elastic moduli is

$$v_{shear}=\sqrt{\frac{E}{3\rho}}, \quad (3)$$

where E is Young's modulus, a measure of the stiffness of an isotropic elastic material; and ρ is the density of the medium.

METHODS

Fatty phantom preparation began with the creation of a 10% porcine gelatin mixture (300 Bloom Pork Gelatin; Gelatin Innovations Inc., Schiller Park, IL, USA) heated to 55°C in a water bath. The desired percentage of refined castor oil was then added to the gelatin mixture with 0.33 cc/L of surfactant (liquid Ultra Ivory®, Procter and Gamble Co., Cincinnati, OH, USA). The mixture was then stirred following the specifications of Madsen. et al (2006). The emulsification was cooled in an ice water bath to roughly 30°C, poured into a cube-shaped mold and refrigerated at 4°C overnight. Prior to scanning, the phantom was removed from its mold and allowed to sit at room temperature for 3 h.

Liver specimens were suspended in cube-shaped molds after a hepatectomy. A porcine gelatin mixture heated to 45°C and subsequently cooled to 30°C was poured into the mold and placed in an ice water bath for approximately 90 min, cooling to a temperature of roughly 15°C. When suspending mouse liver specimens an 8% gelatin mixture was used while a 10% gelatin was used with human liver samples. The solid gelatin phantoms were removed from their respective molds and allowed to rest at room temperature for 10 min prior to scanning.

A GE Logic 9 ultrasound machine (GE Healthcare, Milwaukee, WI, USA) was modified to show vibrational sonoelastographic images in the color-flow mode. An ultrasound transducer (M12L; GE Healthcare, Milwaukee, WI, USA) was connected to the ultrasound machine and was placed on top of the phantom. It is a linear array probe with band width of 5–13 MHz.

Two piston vibration exciters (Model 2706; Brüel & Kjaer, Naerum, Denmark) were placed on each side of the phantom. Two line shaped extensions were mounted on the pistons and their abraded surfaces were pressed on the phantoms with contact regions of 831 cm. The shear wave signals were generated by a two-channel signal generator (Model AFG320; Tektronix, Beaverton, OR, USA) and were amplified equally by a power amplifier (Model 5530; AE Techron, Elkhart, IN, USA), which was connected to the pistons.

See Figure 2 for a depiction of the experimental configuration. The imaged cross-section is parallel to the x-y plane. The transducer and the vibration line sources are in the same plane. The x direction corresponds to the width of the phantom and the y direction corresponds to the depth of the phantom. The shear vibration is along the y axis and the shear wave propagates along the x axis.

The vibrational sources were driven at frequencies offset by 0.35 Hz, creating a CrW. A ROI was selected from each of the sonoelastographic images of CrW propagation through the embedded liver specimens and a projection of the wave image over the axis perpendicular to the stripes was fit to a cosine model based on eqn (1). From the model parameters, a wavelength value and attenuation was derived. Sonoelastographic images gathered from frequencies generated between 100–400 Hz (depending on the size, stiffness and attenuation of the sample) provide the basis for assessing the dispersion of shear velocity estimates. The useful bandwidth and the reference shear wave frequency within the band, depends on the size of and loss in the specimens. Therefore, the reference frequency for shear velocity has value only for comparisons within a similar band of measurements.

RESULTS

In vitro oil/gelatin slurries

To support our basic hypothesis, we found that in comparing fatty castor oil phantoms with pure gelatin slurries, dispersion is higher (0.1 m/s per 100 Hz) and shear velocity is lower (3 m/s) in the fatty phantom relative to the pure gelatin phantom (0 m/s per 100 Hz and 3.5 m/s, respectively), as shown in Figure 3. Error bars give the 95% confidence intervals for the linear fit to slope and reference intercept of the crawling wave data at 5–7 discrete shear wave frequencies between 150 and 350 Hz. Attenuation of shear waves increased from low levels in pure gelatin to nearly 0.9 Np/cm at 40% oil with high dispersion, as shown in Figure 4.

Steatotic vs. lean mouse liver measurements

To further test our hypothesis, fourteen mouse liver specimens (seven lean ob/1 fed a regular diet and seven steatotic ob/ob fed a high fat diet) were scanned *ex vivo*. All animal experiments were performed in accordance with a protocol approved by the University of Rochester Committee on Animal Resources (an IACUC). In ob/obmice, the mean dispersion slope weighted by the inverse of variance of each sample was 0.23 ± 0.04 m/s per 100 Hz, compared with lean mice at 0.16 ± 0.03 m/s per 100 Hz. The average shear velocity was 1.61 ± 0.12 m/s at 260 Hz in ob/ob mice and 1.69 ± 0.17 m/s at 260 Hz in lean mice (Fig. 5a). A paired *t*-test showed the dispersion slope was significantly different ($p < 0.003$) between lean and ob/ob steatotic livers (Fig. 5b). Shear velocity differences were not statistically significant. Histologic analysis of hematoxylin and eosin (H&E) stained sections and Oil Red O staining confirms the absence of steatosis in the lean mice and approximately 65% steatosis in the ob/ob mice (Fig. 6 shows representative samples).

Measurements of human liver explants

Human liver explants were sampled for measurements under a University of Rochester IRB approved protocol with informed consent. Figure 7 depicts the results from four specimens in the 2-D plot of dispersion slope vs. shear speed at a reference frequency. The reference frequency in these cases is 120 Hz, lower than our reference for mouse livers since the human specimens are larger and are covered by lower crawling wave frequencies. The four samples have respective grades of: normal; steatotic with approximately 10% fat but no fibrosis; steatotic with 10% fat and low grade fibrosis; and finally, 35% fat and cirrhosis. These preliminary data confirm our general hypothesis that steatosis will increase

dispersion, from the lowest value of 0.2 m/s per 100 Hz in a normal liver, to 0.55 m/s per 100 Hz in the case with 30%–40% steatosis, plus cirrhosis. Also, the shear velocity is greatest in the sample with cirrhosis, as expected from the results of numerous clinical studies (Sandrin et al. 2003; Castera et al. 2008; Palmeri et al. 2008).

DISCUSSION AND CONCLUSION

Crawling waves can be generated by a pair of sources that create an interference pattern of shear waves. These crawling wave patterns in liver, measured over a band of shear wave frequencies, enables the assessment of the dispersion, or frequency dependence, of shear wave speed and attenuation in the liver. Increasing amounts of fat in the form of steatosis evidently increases the viscosity, or loss term, and this results in increased dispersion of shear wave speed and attenuation.

The successful development of a noninvasive method to measure hepatic steatosis will have widespread clinical applications. Given the morbid obesity epidemic and the associated high incidence of fatty liver disease in the population, an inexpensive and logistically facile ultrasound scan could be employed to serially track disease progression, evaluate the efficacy of lifestyle changes and emerging pharmacologic interventions and guide the rational use of liver biopsies. Other specific patient populations that could benefit from this technology include those with diabetes mellitus type II (70% of whom are estimated to have fatty livers) and potential organ donors for liver transplantation (both living and deceased). Although MRI has been shown to reliably estimate hepatic steatosis (Bydder et al. 2008; Ehman 2009; Salameh et al. 2009), the cost effectiveness and portability of ultrasound are more attractive for widespread clinical applications.

Although not rigorously assessed in our current study, the ability of a single device to simultaneously measure hepatic steatosis and fibrosis is quite attractive. The progression from simple steatosis to NASH is estimated to occur in only 1%–5% of patients (Adams et al. 2005; Liou and Kowdley 2006) but those progressing to NASH are at a significantly higher risk for developing hepatocellular carcinoma (Mori et al. 2004; Bugianesi 2007) and are also more likely to require liver transplantation (Schreuder et al. 2008). Serial imaging of both steatosis and fibrosis would provide valuable clinical information to direct emerging therapeutic interventions designed to slow or halt the progression to end stage liver disease.

Further research is required to determine a number of experimental factors. One question is the minimum percent change in steatosis that can be detected with our crawling wave technique. Another is the ability to maintain accuracy *in vivo*, where the effects of overlying abdominal layers and breathing motion will degrade the estimate of the crawling waves from the Doppler images. Additional experiments are planned to explore these issues.

Acknowledgments

This work was supported by NIH grant 5R01AG02980-04. The authors would like to thank the University of Rochester Medical Center, Department of Transplant Surgery.

REFERENCES

Adams LA, Lymp JF, St Sauver J, Sanderson SO, Lindor KD, Feldstein A, Angulo P. The natural history of nonalcoholic fatty liver disease: A population-based cohort study. Gastroenterology. 2005; 129:113–121. [PubMed: 16012941]

Angulo P. Nonalcoholic fatty liver disease. N Engl J Med. 2002; 346:1221–1231. [PubMed: 11961152]

Blackstock, DT. Fundamentals of physical acoustics, Ch. 9. Wiley; New York: 2000.

Bugianesi E. Non-alcoholic steatohepatitis and cancer. Clin Liver Dis. 2007; 11:191–207. x–xi. [PubMed: 17544979]

Bydder M, Yokoo T, Hamilton G, Middleton MS, Chavez AD, Schwimmer JB, Lavine JE, Sirlin CB. Relaxation effects in the quantification of fat using gradient echo imaging. Magn Reson Imaging. 2008; 26:347–359. [PubMed: 18093781]

Carstensen EL, Parker KJ, Lerner RM. Elastography in the management of liver disease. Ultrasound Med Biol. 2008; 34:1535–1546. [PubMed: 18485568]

Castaneda B, An L, Wu S, Baxter LL, Yao JL, Joseph JV, Hoyt K, Strang J, Rubens DJ, Parker KJ. Prostate cancer detection using crawling wave sonoelastography. Medical Imaging 2009: Ultrasonic Imaging and Signal Processing. Proc. of SPIE. 2009; 7265:726513-1–726513-10.

Castera L, Forns X, Alberti A. Non-invasive evaluation of liver fibrosis using transient elastography. J Hepatol. 2008; 48:835–847. [PubMed: 18334275]

Charlton M. Nonalcoholic fatty liver disease: A review of current understanding and future impact. Clin Gastroenterol Hepatol. 2004; 2:1048–1058. [PubMed: 15625647]

Chen S, Urban MW, Pislaru C, Kinnick R, Zheng Y, Yao A, Greenleaf JF. Shearwave dispersion ultrasound vibrometry (SDUV) for measuring tissue elasticity and viscosity. IEEE Trans Ultrason Ferroelectr Freq Control. 2009; 56:55–62. [PubMed: 19213632]

Debongnie JC, Pauls C, Fievez M, Wibin E. Prospective evaluation of the diagnostic accuracy of liver ultrasonography. Gut. 1981; 22:130–135. [PubMed: 7215943]

Dowman JK, Tomlinson JW, Newsome PN. Pathogenesis of nonalcoholic fatty liver disease. QJM. 2010; 103:71–83. [PubMed: 19914930]

Ehman RL. Science to practice: Can MR elastography be used to detect early steatohepatitis in fatty liver disease? Radiology. 2009; 253:1–3. [PubMed: 19789246]

Foster KJ, Dewbury KC, Griffith AH, Wright R. The accuracy of ultrasound in the detection of fatty infiltration of the liver. Br J Radiol. 1980; 53:440–442. [PubMed: 7388276]

Hessheimer AJ, Parramon D, Guimera A, Erill I, Rimola A, Garcia-Valdecasas JC, Villa R, Fondevila C. A rapid and reliable means of assessing hepatic steatosis *in vivo via* electrical bio-impedance. Transplantation. 2009; 88:716–722. [PubMed: 19741471]

Hoyt K, Castaneda B, Parker KJ. Muscle tissue characterization using quantitative sonoelastography: Preliminary results. IEEE Ultrason Symp. 2007:365–368.

Hoyt K, Castaneda B, Parker KJ. Two-dimensional sonoelastographic shear velocity imaging. Ultrasound Med Biol. 2008; 34:276–288. [PubMed: 17935863]

Hoyt K, Parker KJ, Rubens DJ. Sonoelastographic shear velocity imaging: Experiments on tissue phantom and prostate. IEEE Ultrason Symp. 2006:1686–1689.

Lin K, McLaughlin J, Renzi D, Thomas A. Shear wave speed recovery in sonoelastography using crawling wave data. J Acoust Soc Am. 2010; 128:88–97. [PubMed: 20649204]

Liou I, Kowdley KV. Natural history of nonalcoholic steatohepatitis. J Clin Gastroenterol. 2006; 40(Suppl 1):S11–S16. [PubMed: 16540761]

Longo R, Pollesello P, Ricci C, Masutti F, Kvam BJ, Bercich L, Croce LS, Grigolato P, Paoletti S, de Bernard B, Tiribelli C, Dallapalma L. Proton MR spectroscopy in quantitative *in vivo* determination of fat content in human liver steatosis. J Magn Reson Imaging. 1995; 5:281–285. [PubMed: 7633104]

Madsen EL, Hobson MA, Frank GR, Shi H, Jiang J, Hall TJ, Varghese T, Doyley MM, Weaver JB. Anthropomorphic breast phantoms for testing elastography systems. Ultrasound Med Biol. 2006; 32:857–874. [PubMed: 16785008]

Marchesini G, Brizi M, Morselli-Labate AM, Bianchi G, Bugianesi E, McCullough AJ, Forlani G, Melchionda N. Association of nonalcoholic fatty liver disease with insulin resistance. Am J Med. 1999; 107:450–455. [PubMed: 10569299]

McLaughlin J, Renzi D, Parker K, Wu Z. Shear wave speed recovery using moving interference patterns obtained in sonoelastography experiments. J Acoust Soc Am. 2007; 121:2438–2446. [PubMed: 17471755]

Minervini MI, Ruppert K, Fontes P, Volpes R, Vizzini G, de Vera ME, Gruttadauria S, Miraglia R, Pipitone L, Marsh JW, Marcos A, Gridelli B, Demetris AJ. Liver biopsy findings from healthy

potential living liver donors: Reasons for disqualification, silent diseases and correlation with liver injury tests. J Hepatol. 2009; 50:501–510. [PubMed: 19155086]

Mori S, Yamasaki T, Sakaida I, Takami T, Sakaguchi E, Kimura T, Kurokawa F, Maeyama S, Okita K. Hepatocellular carcinoma with nonalcoholic steatohepatitis. J Gastroenterol. 2004; 39:391–396. [PubMed: 15168253]

Muller M, Gennisson JL, Deffieux T, Tanter M, Fink M. Quantitative viscoelasticity mapping of human liver using supersonic shear imaging: Preliminary *in vivo* feasibility study. Ultrasound Med Biol. 2009; 35:219–229. [PubMed: 19081665]

O'Donnell M, Jaynes ET, Miller JG. Kramers-Kronig relationship between ultrasonic-attenuation and phase-velocity. J Acoust Soc Am. 1981; 69:696–701.

Oestreicher HL. Field and impedance of an oscillating sphere in a viscoelastic medium with an application to biophysics. J Acoust Soc Am. 1951; 23:704–714.

Orescanin M, Insana M. Shear modulus estimation with vibrating needle stimulation. IEEE Trans Ultrason Ferroelectr Freq Control. 2010; 57:1358–1367. [PubMed: 20529711]

Palmeri ML, Wang MH, Dahl JJ, Frinkley KD, Nightingale KR. Quantifying hepatic shear modulus *in vivo* using acoustic radiation force. Ultrasound Med Biol. 2008; 34:546–558. [PubMed: 18222031]

Parker KJ, Doyley MM, Rubens DJ. Imaging the elastic properties of tissue: The 20-year perspective. Phys Med Biol. 2011; 56:R1–R29. [PubMed: 21119234]

Salameh N, Larrat B, Abarca-Quinones J, Pallu S, Dorvillius M, Leclercq I, Fink M, Sinkus R, Van Beers BE. Early detection of steatohepatitis in fatty rat liver by using MR elastography. Radiology. 2009; 253:90–97. [PubMed: 19587308]

Sandrin L, Fourquet B, Hasquenoph JM, Yon S, Fournier C, Mal F, Christidis C, Ziol M, Poulet B, Kazemi F, Beaugrand M, Palau R. Transient elastography: A new noninvasive method for assessment of hepatic fibrosis. Ultrasound Med Biol. 2003; 29:1705–1713. [PubMed: 14698338]

Sarvazyan AP, Rudenko OV, Swanson SD, Fowlkes JB, Emelianov SY. Shear wave elasticity imaging: A new ultrasonic technology of medical diagnostics. Ultrasound Med Biol. 1998; 24:1419–1435. [PubMed: 10385964]

Sasso M, Beaugrand M, de Ledinghen V, Douvin C, Marcellin P, Poupon R, Sandrin L, Miette V. Controlled attenuation parameter (CAP): A novel VCTE guided ultrasonic attenuation measurement for the evaluation of hepatic steatosis: Preliminary study and validation in a cohort of patients with chronic liver disease from various causes. Ultrasound Med Biol. 2010; 36:1825–1835. [PubMed: 20870345]

Schreuder TC, Verwer BJ, van Nieuwkerk CM, Mulder CJ. Nonalcoholic fatty liver disease: An overview of current insights in pathogenesis, diagnosis and treatment. World J Gastroenterol. 2008; 14:2474–2486. [PubMed: 18442193]

Selzner M, Clavien PA. Fatty liver in liver transplantation and surgery. Semin Liver Dis. 2001; 21:105–113. [PubMed: 11296690]

Strassburg CP, Manns MP. Approaches to liver biopsy techniques-Rrevisited. Semin Liver Dis. 2006; 26:318–327. [PubMed: 17051446]

Szabo TL, Wu J. A model for longitudinal and shear wave propagation in viscoelastic media. J Acoust Soc Am. 2000; 107:2437–2446. [PubMed: 10830366]

Tanter M, Bercoff J, Athanasiou A, Deffieux T, Gennisson JL, Montaldo G, Muller M, Tardivon A, Fink M. Quantitative assessment of breast lesion viscoelasticity: Initial clinical results using supersonic shear imaging. Ultrasound Med Biol. 2008; 34:1373–1386. [PubMed: 18395961]

Vuppalanchi R, Chalasani N. Nonalcoholic fatty liver disease and nonalcoholic steatohepatitis: Selected practical issues in their evaluation and management. Hepatology. 2009; 49:306–317. [PubMed: 19065650]

Wang MH, Palmeri ML, Guy CD, Yang L, Hedlund LW, Diehl AM, Nightingale KR. In vivo quantification of liver stiffness in a rat model of hepatic fibrosis with acoustic radiation force. Ultrasound Med Biol. 2009; 35:1709–1721. [PubMed: 19683381]

Wanless IR, Lentz JS. Fatty liver hepatitis (steatohepatitis) and obesity: An autopsy study with analysis of risk factors. Hepatology. 1990; 12:1106–1110. [PubMed: 2227807]

Wu Z, Hoyt K, Rubens DJ, Parker KJ. Sonoelastographic imaging of interference patterns for estimation of shear velocity distribution in biomaterials. J Acoust Soc Am. 2006; 120:535–545. [PubMed: 16875250]

Yoneda M, Suzuki K, Kato S, Fujita K, Nozaki Y, Hosono K, Saito S, Nakajima A. Nonalcoholic fatty liver disease: US-based acoustic radiation force impulse elastography. Radiology. 2010; 256:640–647. [PubMed: 20529989]

Zhang M, Castaneda B, Wu Z, Nigwekar P, Joseph JV, Rubens DJ, Parker KJ. Congruence of imaging estimators and mechanical measurements of viscoelastic properties of soft tissues. Ultrasound Med Biol. 2007; 33:1617–1631. [PubMed: 17604902]

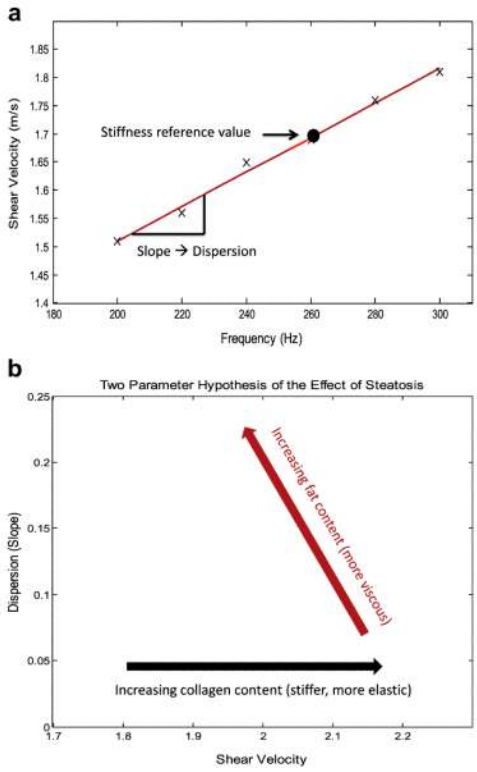

Fig. 1.

A two parameter assessment of liver viscoelastic properties and their dependence on steatosis and fibrosis: (a) shear velocity (vertical axis) is measured over an accessible bandwidth and plotted as a function of frequency (horizontal axis). Regardless of the precise viscoelastic model, the first order fit yields the slope and reference intercept of the dispersion; (b) the results can be placed in a two parameter plot of dispersion slope (vertical axis) and shear velocity at a reference frequency (horizontal axis). Our hypothesis is that increasing fat content in liver will increase the slope of the dispersion measurement.

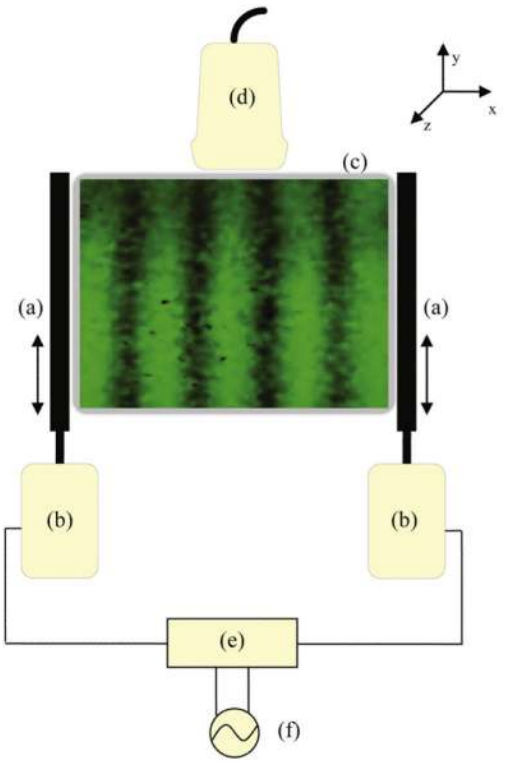

Fig. 2.
Schematic drawing of the experiment set-up. (a) line-shaped contacts; (b) piston vibration exciters; (c) the imaged cross-section of the phantom; (d) ultrasound transducer; (e) amplifier; (f) function generator.

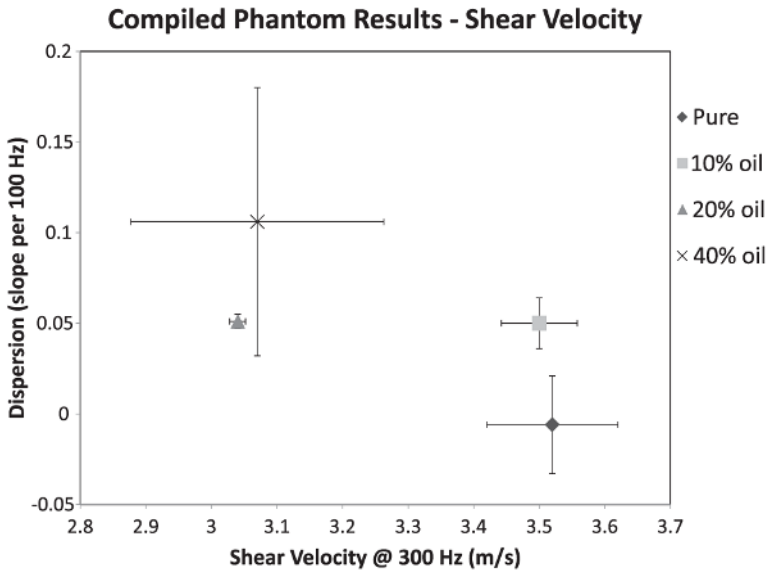

Fig. 3.

Two parameter (shear wave speed and its dispersion slope) plot for phantoms containing a fine suspension of triglycerides (fat) from 0% to 40%. Dispersion tends to increase with fat concentration.

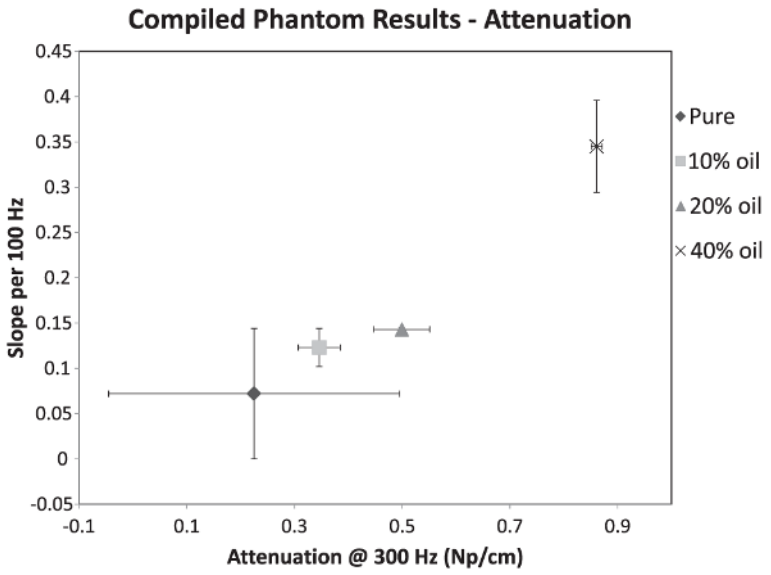

Fig. 4.

Two parameter plot for shear wave attenuation in fatty phantoms. Increasing slope and reference values (at 300 Hz) are found with increasing fat concentration.

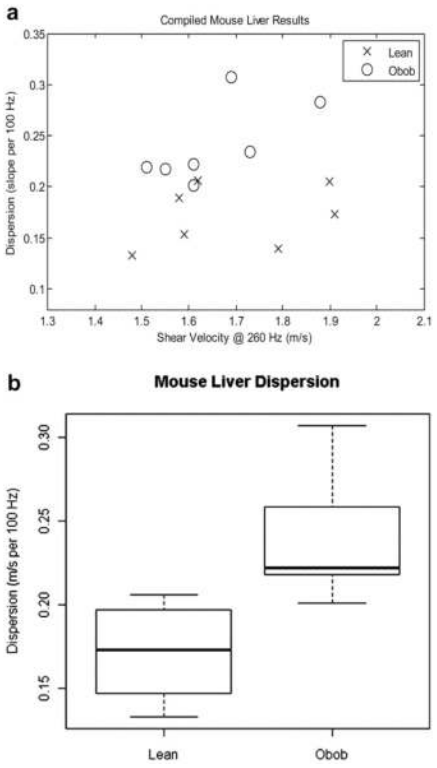

Fig. 5.

(a) Dispersion in mouse livers, lean and steatotic. Vertical axis: dispersion slope; horizontal axis: shear velocity at a reference frequency of 260 Hz. The median standard deviation of the samples in the horizontal and vertical direction is 0.049 for dispersion; 0.127 for velocity. (b) Comparison of lean and obese mouse liver dispersion showing the mean (solid line), standard deviation and range for each group. The difference is significant ($p < 0.003$).

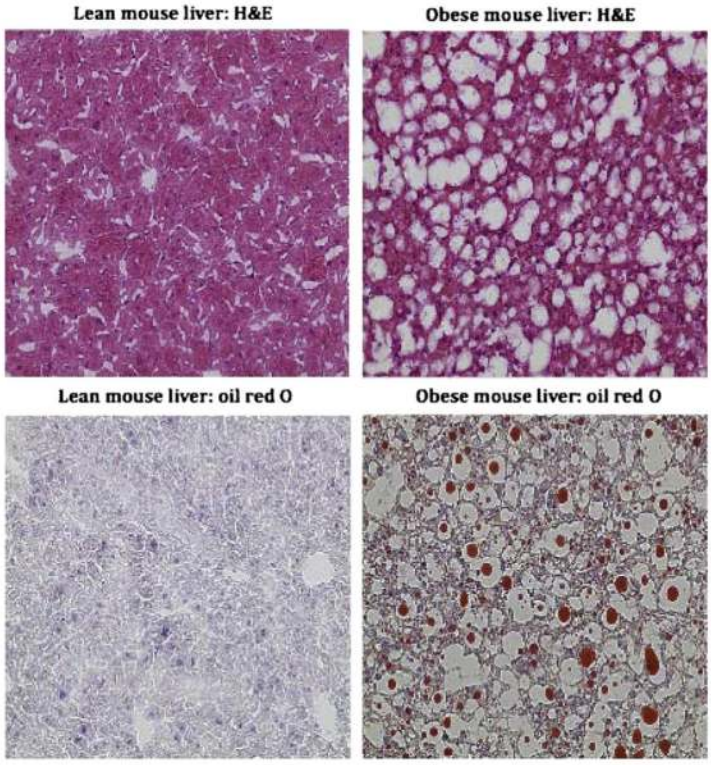

Fig. 6.
H & E and oil red O staining of obese and lean mouse livers.

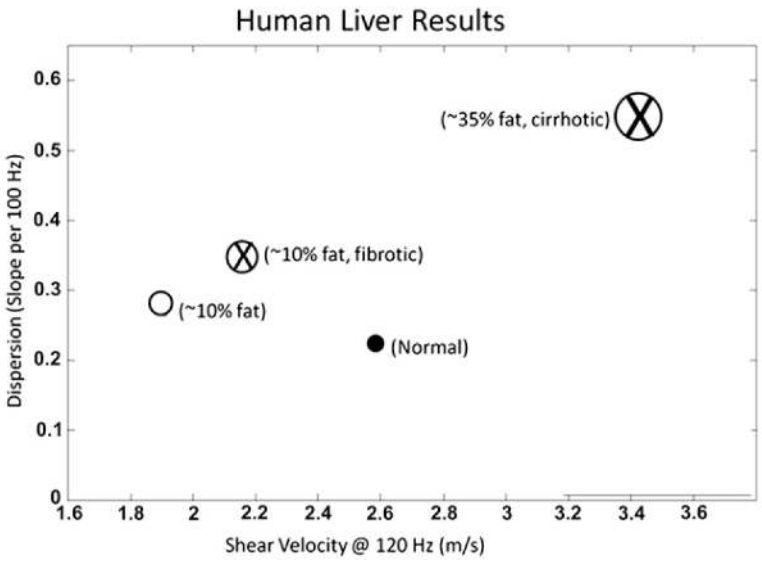

Fig. 7.

Two parameter assessment of dispersion in four human liver specimens, *ex vivo*. The median standard deviation of the samples in the vertical and horizontal direction is 0.23 for dispersion; 0.37 for velocity. The size of the circles indicates fat content. The size of the X indicates fibrosis/cirrhosis staging.